

## Supporting Information

### Supramolecular helix of an oligomeric azapeptide building block containing four $\beta$ -turn structures

Yingdan Zhao,<sup>a</sup> Xiaosheng Yan<sup>a,b</sup> and Yun-Bao Jiang<sup>a,\*</sup>

<sup>a</sup> Department of Chemistry, College of Chemistry and Chemical Engineering, and the  
MOE Key Laboratory of Spectrochemical Analysis and Instrumentation, Xiamen  
University, Xiamen 361005, China

<sup>b</sup> Fujian Provincial Key Laboratory of Innovative Drug Target Research and State Key  
Laboratory of Cellular Stress Biology, School of Pharmaceutical Sciences, Xiamen  
University, Xiamen, Fujian 361102, China.

E-mail: ybjiang@xmu.edu.cn

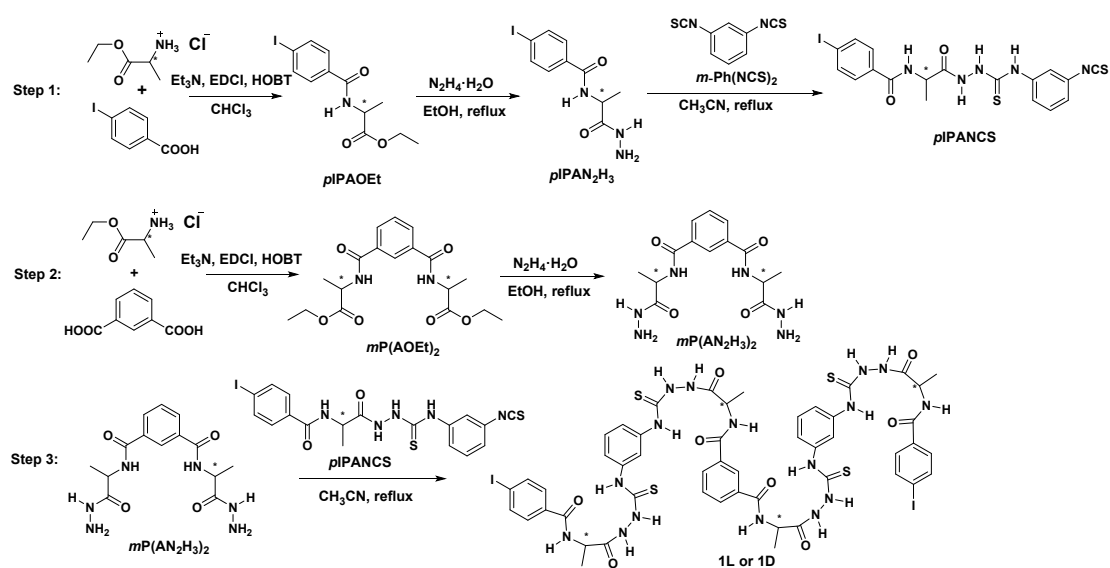
## Content

1. General methods .....	S2
2. Syntheses and characterizations .....	S2
3. Experimental data.....	S6
4. <sup>1</sup> H NMR and <sup>13</sup> C NMR spectra.....	S21

## 1. General methods

$^1\text{H}$  NMR,  $^{13}\text{C}$  NMR and 2D NMR spectra were recorded on Bruker AV500 MHz, AV600 MHz or AV850 MHz spectrometer in dimethyl sulfoxide- $\text{D}_6$  ( $\text{DMSO-}d_6$ ), acetonitrile- $\text{D}_3$  ( $\text{CD}_3\text{CN}$ ) or their mixed solvents. High-resolution mass spectra (HR-MS) were obtained on a Bruker En Apex ultra 7.0 FT-MS. Absorption spectra were recorded on a Thermo Scientific Evolution 300 UV/Vis spectrophotometer. CD spectra were recorded with a JASCO J-1500 spectrometer. DLS data were collected on Malvern Zetasizer Nano-ZS90. SEM experiments were conducted on Hitachi S-4800 scanning electron microscope.

## 2. Syntheses and characterizations



**Scheme S1.** Syntheses of **1L** and **1D**.

**pIPAN<sub>2</sub>H<sub>3</sub>**: *p*-Iodobenzoic acid (2.47 g, 10.0 mmol) was added to 60 mL  $\text{CHCl}_3$ , followed by the gradual addition of 1.5 mL  $\text{Et}_3\text{N}$  under the ice bath to obtain transparent solution. Then EDCI (2.11 g, 11.0 mmol) and HOBT (1.48 g, 11.0 mmol) were added and stirred for 30 min. L-or D-AOEt·HCl (1.50 g, 10.0 mmol) was added to the above solution. The reaction mixture was stirred at room temperature for 12 h. The solvent was removed by evaporated *in vacuo*, 20 mL ethyl acetate and 20 mL pure water were added in turn, and the organic phase was washed with dilute  $\text{NH}_3\cdot\text{H}_2\text{O}$  (0.1 M), dilute

HCl (0.1 M) and saturated NaCl solution for 3 times in turn, then was dried by anhydrous Na<sub>2</sub>SO<sub>4</sub>. The solvent was removed by evaporated *in vacuo* to afford white solid **pIPAOEt**. Next, excess N<sub>2</sub>H<sub>4</sub>·H<sub>2</sub>O (85%, 3.0 mL) was added to **pIPAOEt** in EtOH (50 mL) and the mixture was refluxed for 12 hours. Filtrating to remove the solvent, and the crude product was washed with EtOH and Et<sub>2</sub>O several times to get white solid product **pIPAN<sub>2</sub>H<sub>3</sub>** (60% yield).

**pIPANCS**: **pIPAN<sub>2</sub>H<sub>3</sub>** (0.333 g, 1.0 mmol) was gradually added to excess *m*-phenyldiisothiocyanate (0.384 g, 2.5 mmol) in CH<sub>3</sub>CN (50 mL) and then refluxed for 24 h. The solvent was removed by filtration, and the crude product was washed with hot CH<sub>3</sub>CN and Et<sub>2</sub>O for several times, affording pure white solid product **pIPANCS** (50% yield).

**mP(AN<sub>2</sub>H<sub>3</sub>)<sub>2</sub>**: Isophthalic acid (1.67 g, 10.0 mmol) was added to 60 mL CHCl<sub>3</sub>, and gradually add 3 mL Et<sub>3</sub>N in the ice bat. Then EDCI (4.22 g, 22.0 mmol) and HOBT (2.97 g, 22.0 mmol) were added and stirred in the ice bath for 30 min. L-or D-AOEt·HCl (3.00 g, 10.0 mmol) was added to the above solution. The reaction mixture was stirred at room temperature for 12 h. The solvent was removed by evaporated *in vacuo*, 20 mL ethyl acetate and 20 mL pure water were added in turn, and the organic phase was washed with dilute NH<sub>3</sub>·H<sub>2</sub>O (0.1 M), dilute HCl (0.1 M) and saturated NaCl solution for 3 times in turn, and was dried by anhydrous Na<sub>2</sub>SO<sub>4</sub>. The solvent was removed by evaporated *in vacuo*, affording a white solid **mP(AOEt)<sub>2</sub>**. Excess N<sub>2</sub>H<sub>4</sub>·H<sub>2</sub>O (85%, 3.0 mL) was added to **mP(AOEt)<sub>2</sub>** in EtOH (50 mL) and the mixture was refluxed for 12 hours. Filtrating to remove the solvent, and the crude product was washed with EtOH and Et<sub>2</sub>O several times, producing white solid product **mP(AN<sub>2</sub>H<sub>3</sub>)<sub>2</sub>** (60% yield).

**1L**: **mP(AN<sub>2</sub>H<sub>3</sub>)<sub>2</sub>** (0.033 g, 0.1 mmol) was gradually added to **pIPANCS** (0.115 g, 0.22 mmol) dropwise in 30 mL CH<sub>3</sub>CN and then refluxed for 48 h. The solvent was removed by filtration, and the crude product was washed with hot CH<sub>3</sub>CN and Et<sub>2</sub>O for several times, producing pure white solid product **1L** (67% yield). **1D** was similarly synthesized.

According to similar synthetic routes for **1L**, **2L-5L** (Fig. 1) were obtained. Replacing *p*-iodobenzoic acid with benzoic acid to generate **2L**; replacing the isophthalic acid with

terephthalic acid leads to **3L**; replacing *m*-phenyldiisothiocyanate with *p*-phenyldiisothiocyanate leads to **4L**; replacing isophthalic acid and *m*-phenyldiisothiocyanate with terephthalic acid and *p*-phenyldiisothiocyanate leads to **5L**.

**1L**:  $^1\text{H}$  NMR (500 MHz, DMSO- $d_6$ )  $\delta$  (ppm) 10.40 (s, 1H), 9.73 (s, 1H), 9.25 (s, 1H), 8.99 (s, 1H), 7.89 (d,  $J$  = 8.2 Hz, 2H), 7.68 (d,  $J$  = 8.3 Hz, 2H), 7.65 (d,  $J$  = 5.8 Hz, 2H), 7.35 (t,  $J$  = 7.7 Hz, 2H), 7.16 (t,  $J$  = 7.1 Hz, 1H), 4.32 (s, 1H), 1.39 (d,  $J$  = 6.9 Hz, 3H).  $^{13}\text{C}$  NMR (151 MHz, DMSO- $d_6$ )  $\delta$  (ppm) 180.19, 171.82, 166.93, 138.97, 137.24, 133.71, 132.66, 130.80, 129.75, 128.52, 127.70, 126.98, 121.35, 99.60, 49.25, 48.97, 16.92, 16.62. HRMS (ESI): calcd for  $[\text{C}_{50}\text{H}_{52}\text{I}_2\text{N}_{16}\text{O}_8\text{S}_4\text{Na}]^+$ : 1409.1018, found: 1409.1021.

**1D**:  $^1\text{H}$  NMR (500 MHz, DMSO- $d_6$ )  $\delta$  10.40 (s, 4H), 9.75 (s, 4H), 9.31 (s, 4H), 8.97 (s, 4H), 8.41 (s, 1H), 8.03 (d,  $J$  = 6.5 Hz, 3H), 7.88 (d,  $J$  = 7.8 Hz, 4H), 7.71 (d,  $J$  = 7.0 Hz, 4H), 7.61 (s, 1H), 7.45 (s, 2H), 7.31 (s, 3H), 4.44 (s, 2H), 4.31 (s, 2H), 1.41 (d,  $J$  = 11.1 Hz, 11H).  $^{13}\text{C}$  NMR (151 MHz, DMSO- $d_6$ )  $\delta$  (ppm) 180.20, 171.83, 166.94, 138.98, 137.25, 133.71, 132.69, 130.82, 129.76, 128.53, 127.71, 127.00, 121.36, 99.59, 49.25, 16.93, 16.64. HRMS (ESI): calcd for  $[\text{C}_{50}\text{H}_{52}\text{I}_2\text{N}_{16}\text{O}_8\text{S}_4\text{Na}]^+$ : 1409.1018, found: 1409.1019.

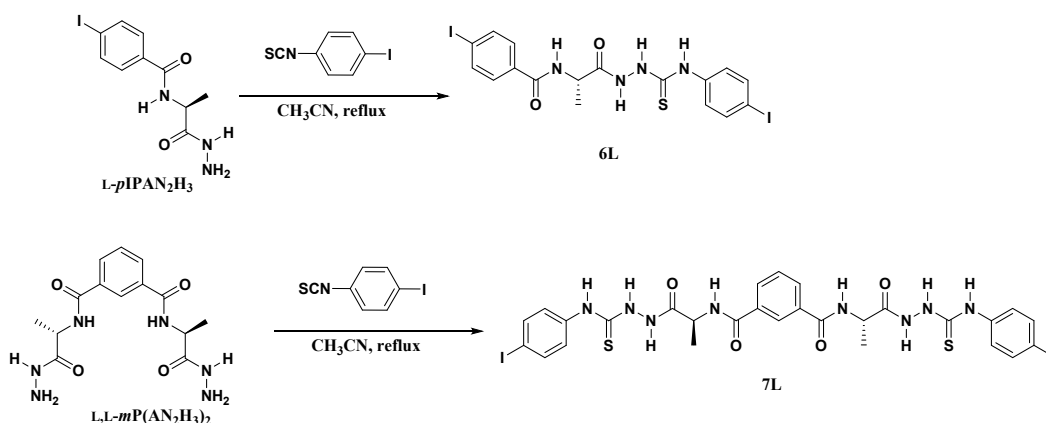
**2L**:  $^1\text{H}$  NMR (500 MHz, DMSO- $d_6$ )  $\delta$  (ppm) 10.39 (s, 4H), 9.73 (s, 4H), 9.36 (s, 2H), 8.89 (s, 3H), 8.41 (s, 1H), 8.03 (d,  $J$  = 7.6 Hz, 3H), 7.92 (d,  $J$  = 7.4 Hz, 4H), 7.61 (d,  $J$  = 7.4 Hz, 1H), 7.53 (t,  $J$  = 7.2 Hz, 2H), 7.48 (t,  $J$  = 7.4 Hz, 4H), 7.42 (s, 2H), 7.31 (d,  $J$  = 6.9 Hz, 3H), 4.39 (d,  $J$  = 55.2 Hz, 4H), 1.41 (t,  $J$  = 8.1 Hz, 12H).  $^{13}\text{C}$  NMR (214 MHz, DMSO- $d_6$ )  $\delta$  (ppm) 180.30, 171.81, 167.00, 138.91, 133.68, 133.19, 131.68, 130.78, 128.49, 128.32, 127.77, 126.95, 121.46, 48.91, 16.90, 16.59. HRMS (ESI): calcd for  $[\text{C}_{50}\text{H}_{54}\text{N}_{16}\text{O}_8\text{S}_4\text{Na}]^+$ : 1157.3086, found: 1157.3086.

**3L**:  $^1\text{H}$  NMR (500 MHz, DMSO- $d_6$ )  $\delta$  (ppm) 10.40 (s, 4H), 9.73 (s, 4H), 9.28 (s, 4H), 8.98 (s, 4H), 7.97 (d,  $J$  = 9.5 Hz, 6H), 7.86 (dd,  $J$  = 8.0, 3.2 Hz, 4H), 7.67 (d,  $J$  = 8.0 Hz, 4H), 7.58 (s, 9H), 4.34 (s, 4H), 1.40 (d,  $J$  = 7.0 Hz, 12H).  $^{13}\text{C}$  NMR (214 MHz, DMSO- $d_6$ )  $\delta$  (ppm) 180.20, 171.85, 166.84, 138.96, 137.23, 135.93, 132.62, 129.73, 127.68, 121.43, 99.59, 49.22, 16.68. HRMS (ESI): calcd for  $[\text{C}_{50}\text{H}_{52}\text{I}_2\text{N}_{16}\text{O}_8\text{S}_4\text{Na}]^+$ :

1409.1019, found: 1409.1019.

**4L:**  $^1\text{H}$  NMR (500 MHz,  $\text{DMSO-}d_6$ )  $\delta$  (ppm) 10.41 (s, 4H), 9.76 (s, 4H), 9.35 (s, 4H), 8.98 (s, 4H), 8.07 (s, 1H), 8.00 (s, 8H), 7.95 (s, 1H), 7.88 (d,  $J = 8.1$  Hz, 1H), 7.70 (d,  $J = 8.0$  Hz, 1H), 7.31 (s, 6H), 4.38 (s, 4H), 1.41 (d,  $J = 5.7$  Hz, 12H).  $^{13}\text{C}$  NMR (214 MHz,  $\text{DMSO-}d_6$ )  $\delta$  (ppm) 180.17, 171.83, 166.96, 137.21, 135.82, 133.88, 132.79, 130.65, 129.61, 128.34, 127.06, 124.35, 124.07, 99.56, 49.21, 16.89, 16.61. HRMS (ESI): calcd for  $[\text{C}_{50}\text{H}_{52}\text{I}_2\text{N}_{16}\text{O}_8\text{S}_4\text{Na}]^+$ : 1409.1019, found: 1409.1005.

**5L:**  $^1\text{H}$  NMR (500 MHz,  $\text{DMSO-}d_6$ )  $\delta$  (ppm) 10.39 (s, 4H), 9.72 (s, 4H), 9.31 (s, 4H), 8.98 (s, 4H), 8.41 (s, 2H), 8.02 (s, 3H), 7.85 (d,  $J = 8.3$  Hz, 3H), 7.67 (d,  $J = 6.9$  Hz, 4H), 7.58 (s, 11H), 4.43 (s, 4H), 1.41 (dd,  $J = 13.2, 7.8$  Hz, 12H).  $^{13}\text{C}$  NMR (214 MHz,  $\text{DMSO-}d_6$ )  $\delta$  (ppm) 180.17, 171.84, 166.82, 137.20, 135.79, 132.81, 129.59, 127.59, 124.06, 99.54, 49.18, 16.63. HRMS (ESI): calcd for  $[\text{C}_{50}\text{H}_{52}\text{I}_2\text{N}_{16}\text{O}_8\text{S}_4\text{Na}]^+$ : 1409.1019, found: 1409.1014.



**Scheme S2.** Syntheses of **6L** and **7L**.

**6L:** L-*p*IPAN<sub>2</sub>H<sub>3</sub> (0.333 g, 1.0 mmol) was gradually added to 4-iodophenyl isothiocyanate (0.261 g, 1 mmol) dropwise in 50 mL CH<sub>3</sub>CN and then refluxed for 12 h. The solvent was removed by filtration, and the crude product was washed with hot CH<sub>3</sub>CN and Et<sub>2</sub>O for several times to afford pure white solid product **6L** (81% yield).

**7L:** L,L-*m*P(AN<sub>2</sub>H<sub>3</sub>)<sub>2</sub> (0.336 g, 1.0 mmol) was gradually added to 4-iodophenyl isothiocyanate (0.574 g, 2.2 mmol) dropwise in 50 mL CH<sub>3</sub>CN and then refluxed for

12 h. The solvent was removed by filtration, and the crude product was washed with hot CH<sub>3</sub>CN and Et<sub>2</sub>O for several times to afford pure white solid product **7L** (88% yield).

**6L**: <sup>1</sup>H NMR (500 MHz, DMSO-*d*<sub>6</sub>) δ (ppm) 10.41 (s, 1H), 9.83 (s, 1H), 9.28 (s, 1H), 9.00 (s, 1H), 7.90 (d, *J* = 8.2 Hz, 2H), 7.69 (t, *J* = 7.6 Hz, 4H), 7.54 (s, 2H), 4.30 (s, 1H), 1.39 (d, *J* = 7.0 Hz, 3H). <sup>13</sup>C NMR (214 MHz, DMSO-*d*<sub>6</sub>) δ (ppm) 179.95, 171.80, 166.99, 138.94, 137.22, 136.85, 132.63, 129.58, 126.02, 99.59, 89.23, 49.25, 16.48. HRMS (ESI): calcd for [C<sub>17</sub>H<sub>16</sub>I<sub>2</sub>N<sub>4</sub>O<sub>2</sub>SNa]<sup>+</sup>: 616.8970, found: 616.8962.

**7L**: <sup>1</sup>H NMR (500 MHz, DMSO-*d*<sub>6</sub>) δ (ppm) 10.44 (s, 2H), 9.85 (s, 2H), 9.32 (s, 2H), 9.06 (s, 2H), 8.41 (s, 1H), 8.06 (d, *J* = 6.5 Hz, 2H), 7.65 (t, *J* = 11.6 Hz, 6H), 7.56 (s, 4H), 4.38 (s, 2H), 1.42 (d, *J* = 5.0 Hz, 6H). <sup>13</sup>C NMR (214 MHz, DMSO-*d*<sub>6</sub>) δ (ppm) 180.18, 171.87, 167.09, 139.03, 133.74, 130.61, 128.31, 128.17, 127.24, 124.86, 124.20, 49.10, 16.72. HRMS (ESI): calcd for [C<sub>28</sub>H<sub>28</sub>I<sub>2</sub>N<sub>8</sub>O<sub>4</sub>S<sub>2</sub>Na]<sup>+</sup>: 880.9657, found: 880.9637.

### 3. Experimental data

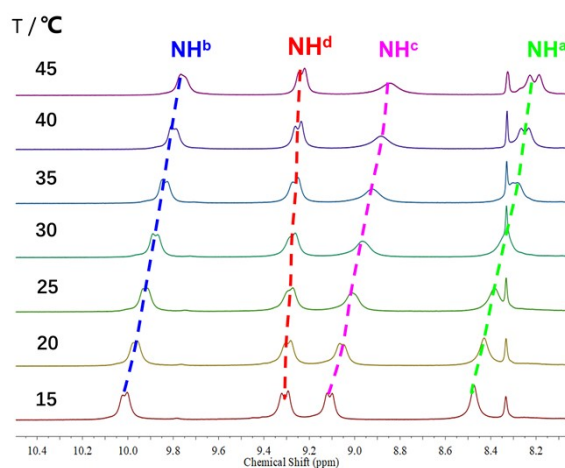


**Figure S1.** Temperature-dependent partial <sup>1</sup>H NMR spectra of -NH protons of **1L** in 90:10 (v/v) CD<sub>3</sub>CN/DMSO-*d*<sub>6</sub> mixture. [**1L**] = 2 mM.

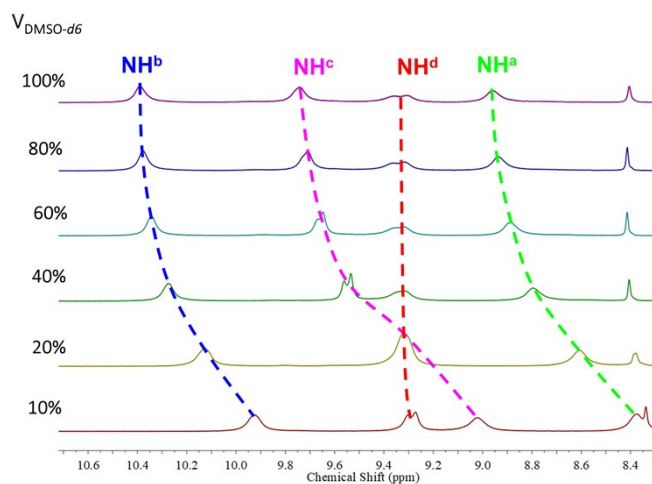


**Figure S2.** Partial  $^1\text{H}$  NMR spectra of -NH protons of **1L** in  $\text{CD}_3\text{CN}/\text{DMSO-}d_6$  mixtures of varying volume fraction of  $\text{DMSO-}d_6$  (500 MHz, 298 K).  $[\mathbf{1L}] = 2 \text{ mM}$ .

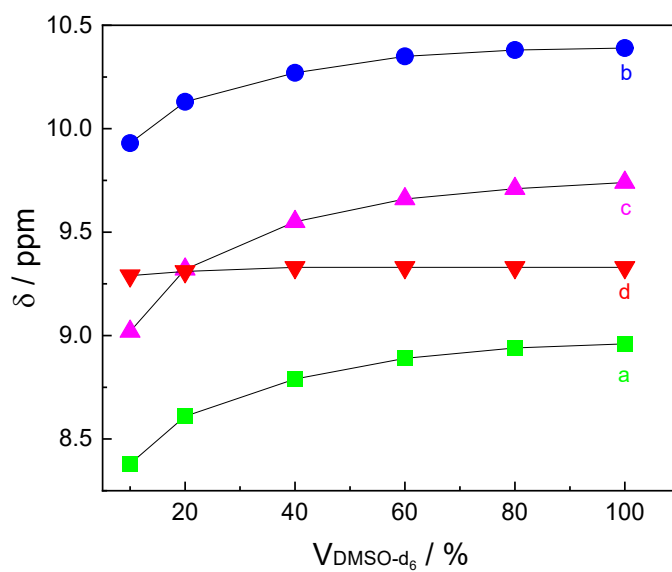


**Figure S3.** Influence on resonances of -NH protons of **1L** in  $\text{CD}_3\text{CN}/\text{DMSO-}d_6$  mixture by volume fraction of  $\text{DMSO-}d_6$  (500 MHz, 298 K).  $[\mathbf{1L}] = 2 \text{ mM}$ .

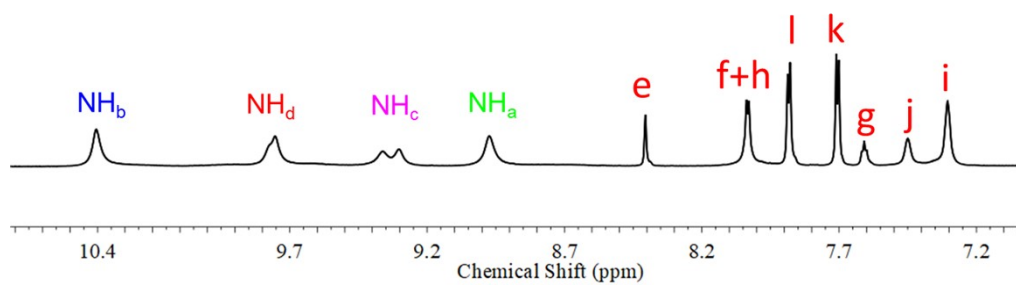


**Figure S4.** Partial  $^1\text{H}$  NMR spectrum of **1L** in  $\text{DMSO-}d_6$ . [**1L**] = 2 mM.

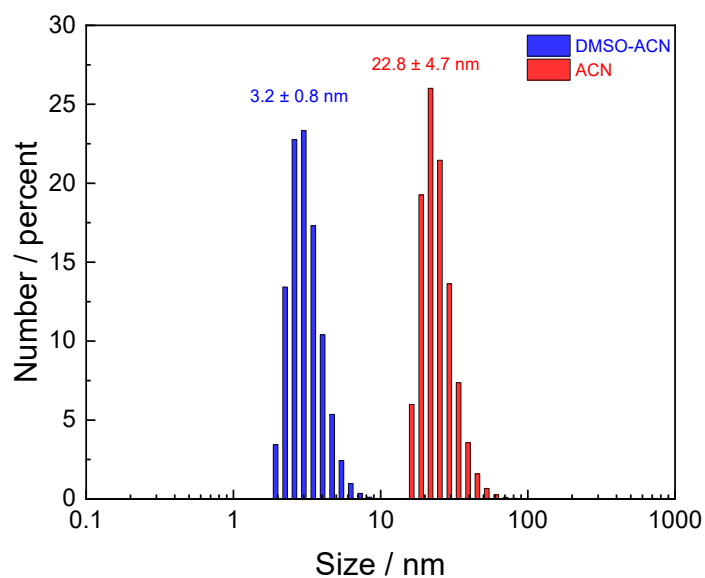


**Figure S5.** Hydrodynamic diameters of **1L** in 1:199 (v/v)  $\text{DMSO}/\text{CH}_3\text{CN}$  and in  $\text{CH}_3\text{CN}$  measured by dynamic light scattering. [**1L**] = 5  $\mu\text{M}$ .



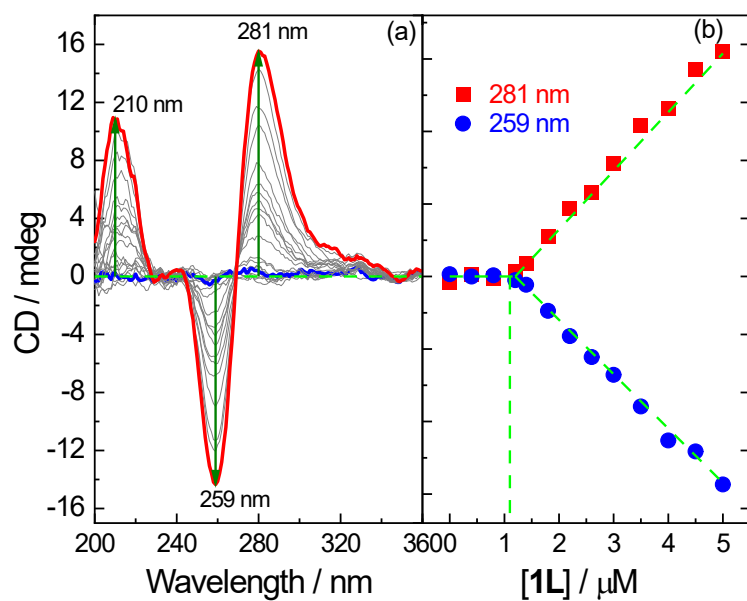


**Figure S6.** (a) Concentration-dependent CD spectra of **1L** in  $\text{CH}_3\text{CN}$  and (b) plots of CD signals at 259 nm and 280 nm versus concentration of **1L** over 0 to 5  $\mu\text{M}$ .

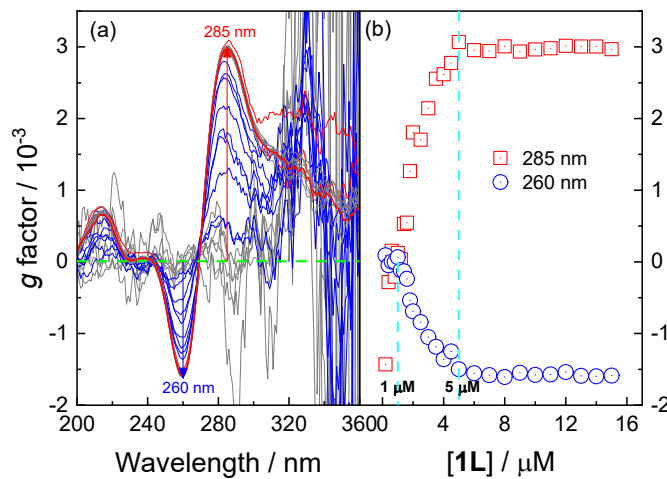


**Figure S7.** (a) Wavelength profiles of g factor of **1L** of increasing concentration in  $\text{CH}_3\text{CN}$  and (b) plots of g factors at 285 nm and 260 nm versus concentration of **1L** over 0 to 15  $\mu\text{M}$ .

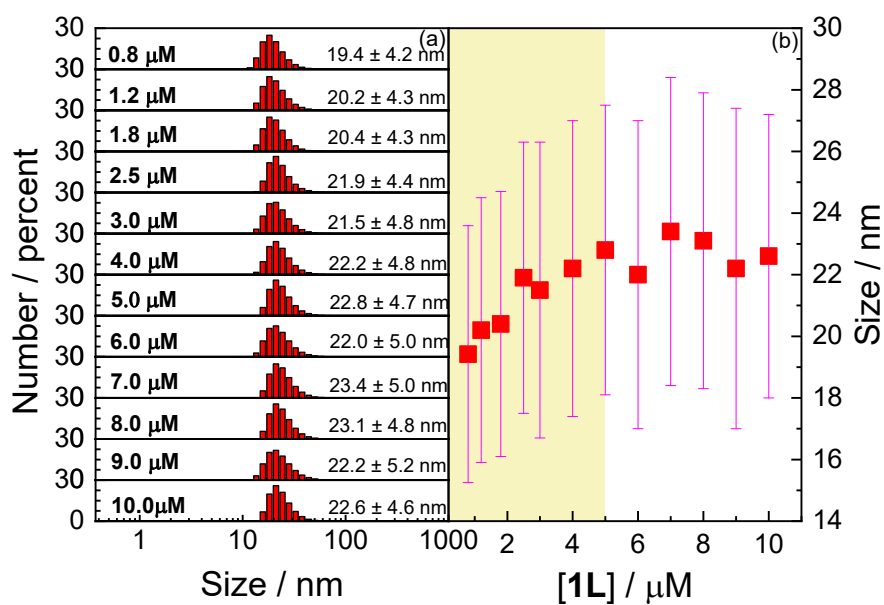


**Figure S8.** (a) DLS hydrodynamic diameters of **1L** of increasing concentration in  $\text{CH}_3\text{CN}$  and (b) plots of hydrodynamic diameter versus concentration of **1L**.  $[1\text{L}] = 0 - 10 \mu\text{M}$ .

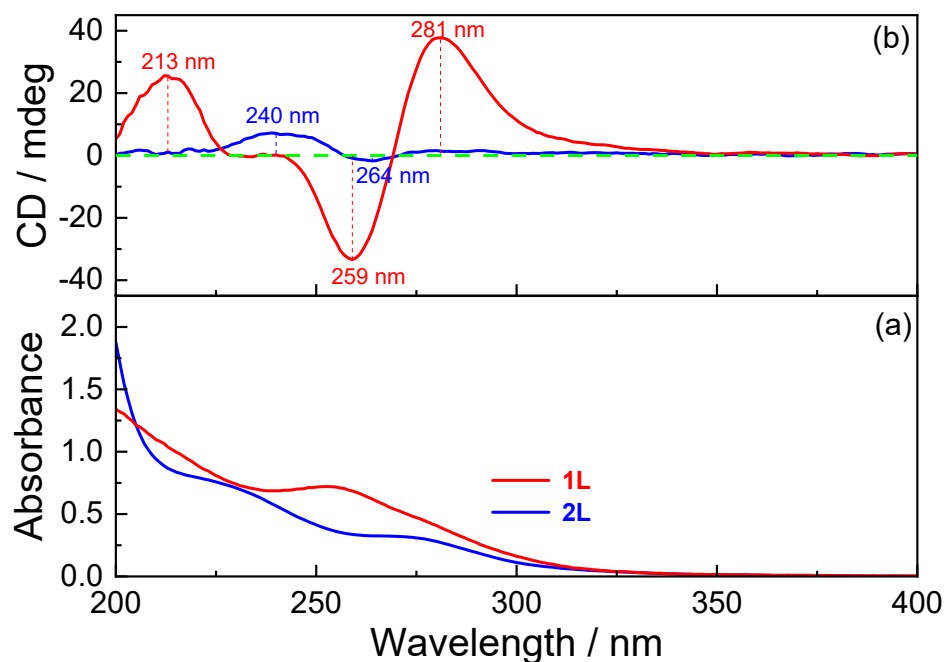


**Figure S9.** Absorption (a) and CD (b) spectra of **1L** (red line) and **2L** (blue line) in  $\text{CH}_3\text{CN}$ .  $[1\text{L}] = [2\text{L}] = 10 \mu\text{M}$ .

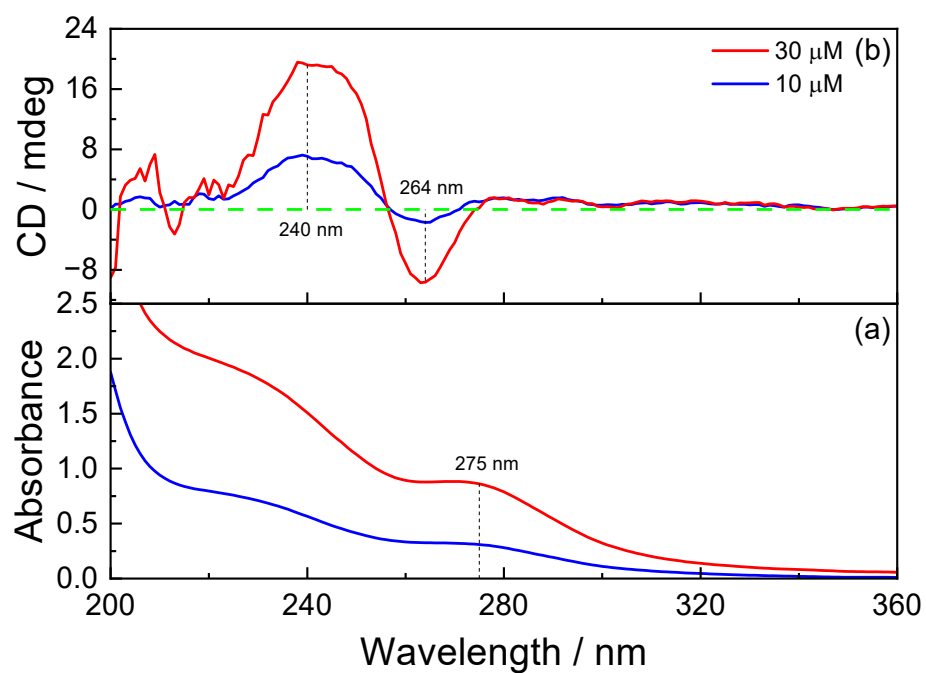


**Figure S10.** Absorption (a) and CD (b) spectra of **2L** of 10 and 30  $\mu\text{M}$  in  $\text{CH}_3\text{CN}$ .

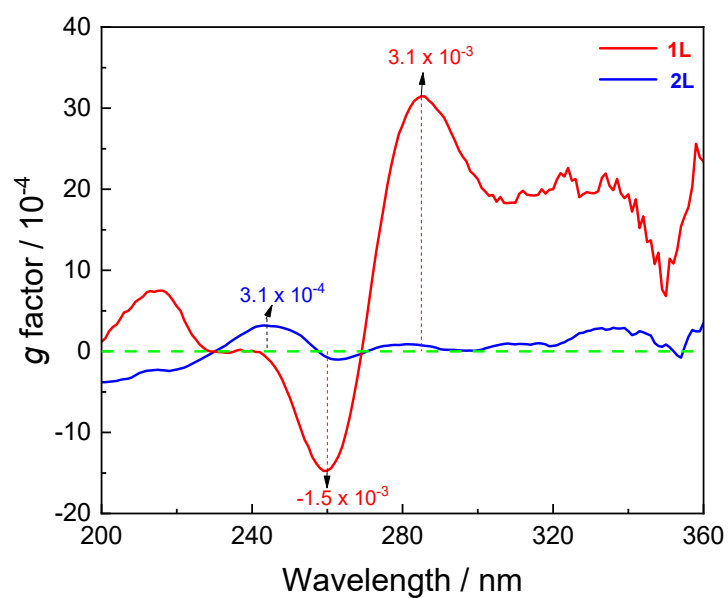


**Figure S11.** Wavelength profiles of g factors of **1L** (red line) and **2L** (blue line) in  $\text{CH}_3\text{CN}$ .  $[\mathbf{1L}] = [\mathbf{2L}] = 10 \mu\text{M}$ .

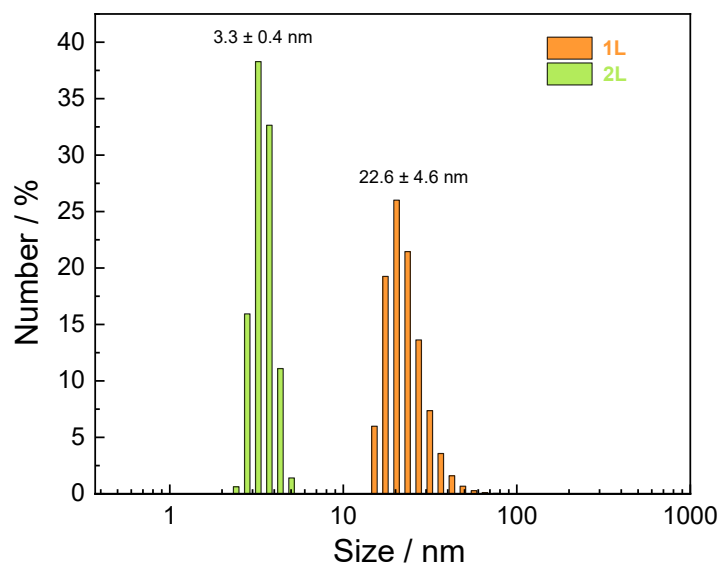


**Figure S12.** Hydrodynamic diameters of **1L** and **2L** in  $\text{CH}_3\text{CN}$  measured by dynamic light scattering.  $[\mathbf{1L}] = [\mathbf{2L}] = 10 \mu\text{M}$ .

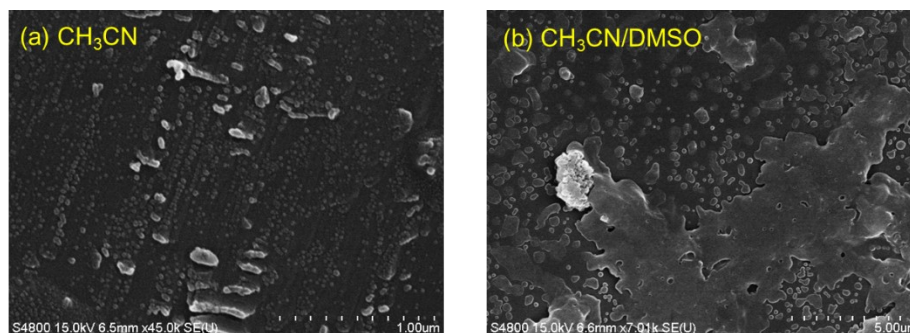


**Figure S13.** SEM images of air-dried samples of **2L** in  $\text{CH}_3\text{CN}$  and 1:199 (v/v) DMSO/ $\text{CH}_3\text{CN}$  on platinum coated silicon wafers.  $[\mathbf{2L}] = 10 \mu\text{M}$ .

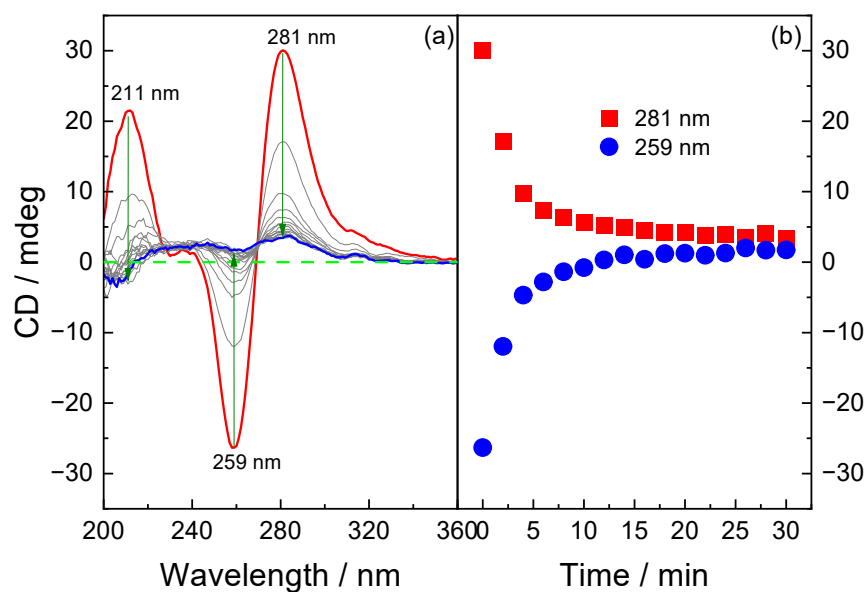


**Figure S14.** (a) Time-dependent CD spectra and (b) CD signals at 281 nm and 259 nm of **1L** in CH<sub>3</sub>CN with 20% by volume H<sub>2</sub>O. [**1L**] = 8 μM.

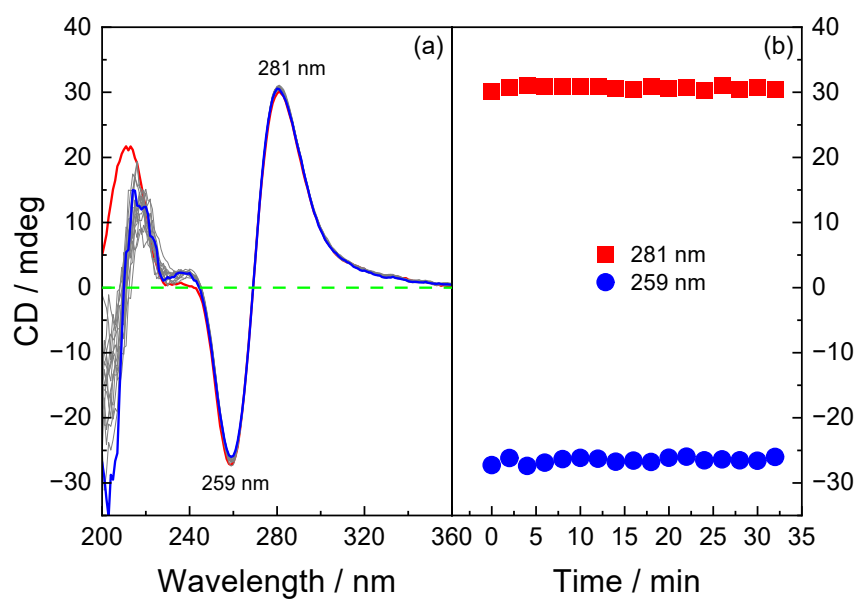


**Figure S15.** (a) Time-dependent CD spectra and (b) CD signals at 281 nm and 259 nm of **1L** in CH<sub>3</sub>CN with 20% by volume THF. [**1L**] = 8 μM.

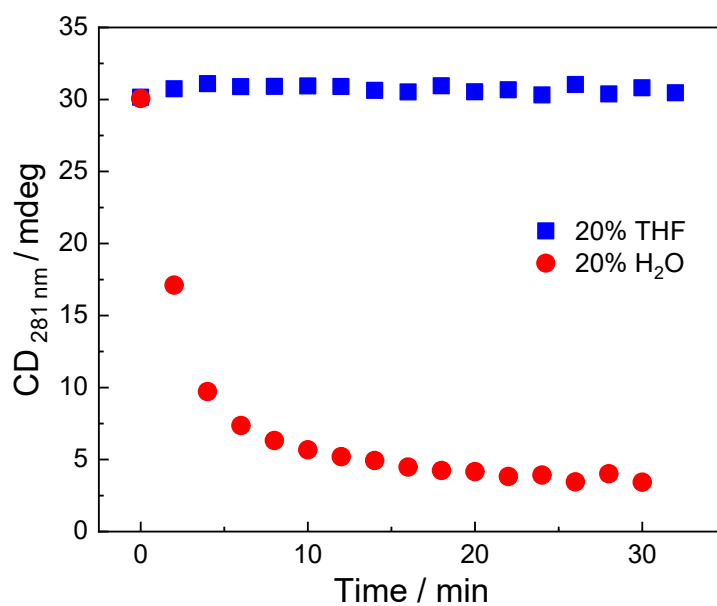


**Figure S16.** Time profiles of CD signal at 281 nm of **1L** in CH<sub>3</sub>CN with 20% volume fraction of THF and H<sub>2</sub>O. [**1L**] = 8  $\mu$ M.

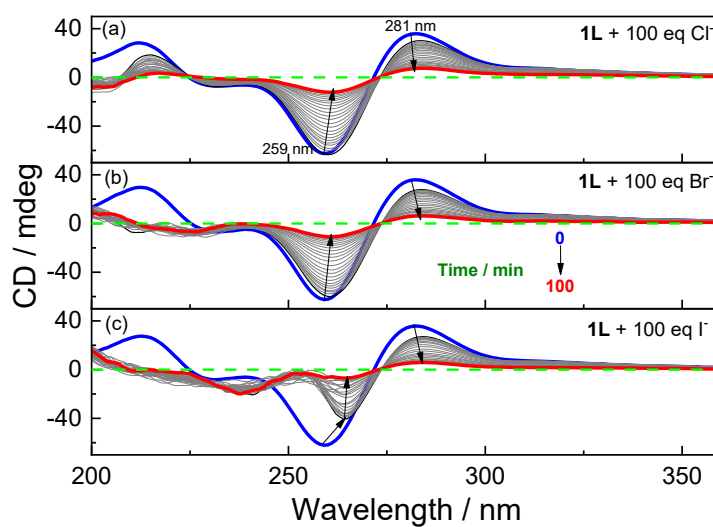


**Figure S17.** Time-dependent CD spectra of **1L** in the presence of 100 eq of Cl<sup>-</sup> (a), Br<sup>-</sup> (b) and I<sup>-</sup> (c) in CH<sub>3</sub>CN. [**1L**] = 10  $\mu$ M, [I<sup>-</sup>] = [Br<sup>-</sup>] = [Cl<sup>-</sup>] = 1000  $\mu$ M. I<sup>-</sup>, Br<sup>-</sup> and Cl<sup>-</sup> exist as their *n*-Bu<sub>4</sub>N<sup>+</sup> salts.

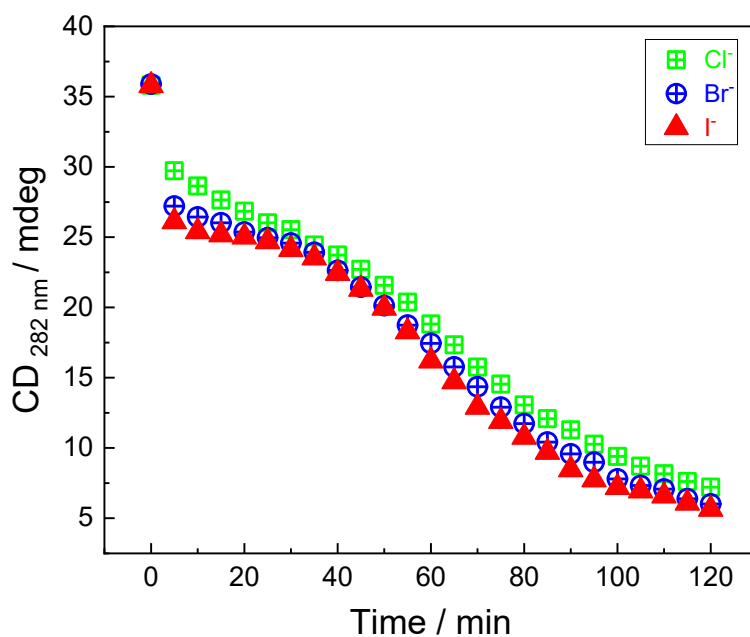


**Figure S18.** Time profiles of CD signal at 282 nm of **1L** in the presence of 100 eq I<sup>-</sup>, Br<sup>-</sup> and Cl<sup>-</sup> in CH<sub>3</sub>CN. [**1L**] = 10 μM, [I<sup>-</sup>] = [Br<sup>-</sup>] = [Cl<sup>-</sup>] = 1000 μM. I<sup>-</sup>, Br<sup>-</sup> and Cl<sup>-</sup> exist as their (*n*-Bu)<sub>4</sub>N<sup>+</sup> salts.

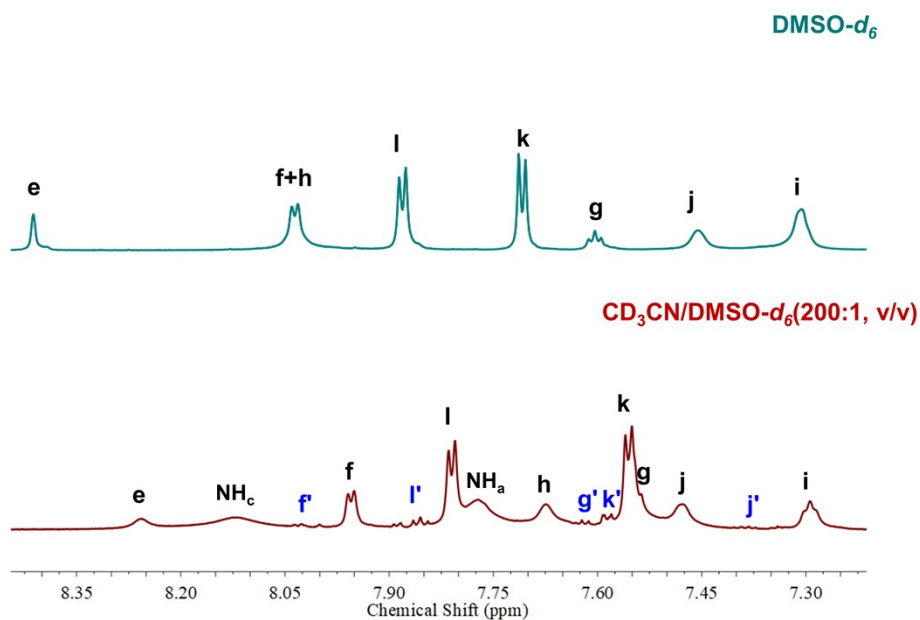


**Figure S19.** Partial <sup>1</sup>H NMR spectra of **1L** in DMSO-*d*<sub>6</sub> and in 200:1 (v/v) CD<sub>3</sub>CN/DMSO-*d*<sub>6</sub> mixture (850 MHz, 25 °C). H<sup>f</sup>, H<sup>l</sup>, H<sup>g</sup>, H<sup>k</sup> and H<sup>j</sup> are those from the oligomers of **1L**. Numbering of protons is shown in Figure 1a. [**1L**] = 200 μM.

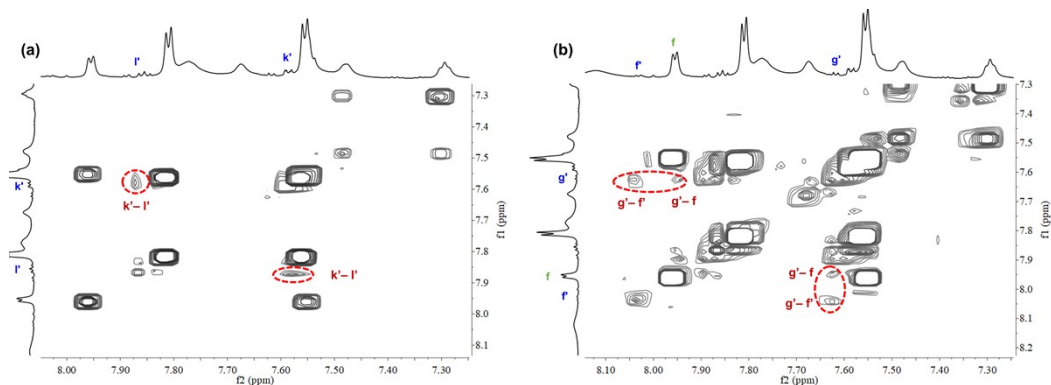


**Figure S20.** Expanded 2D COSY spectra of couplings between protons in phenyl rings in **1L** in 200:1 (v/v) CD<sub>3</sub>CN/DMSO-*d*<sub>6</sub> mixture (850 MHz, 25 °C). Numbering of protons is given in Figure 1a. [**1L**] = 200 μM.

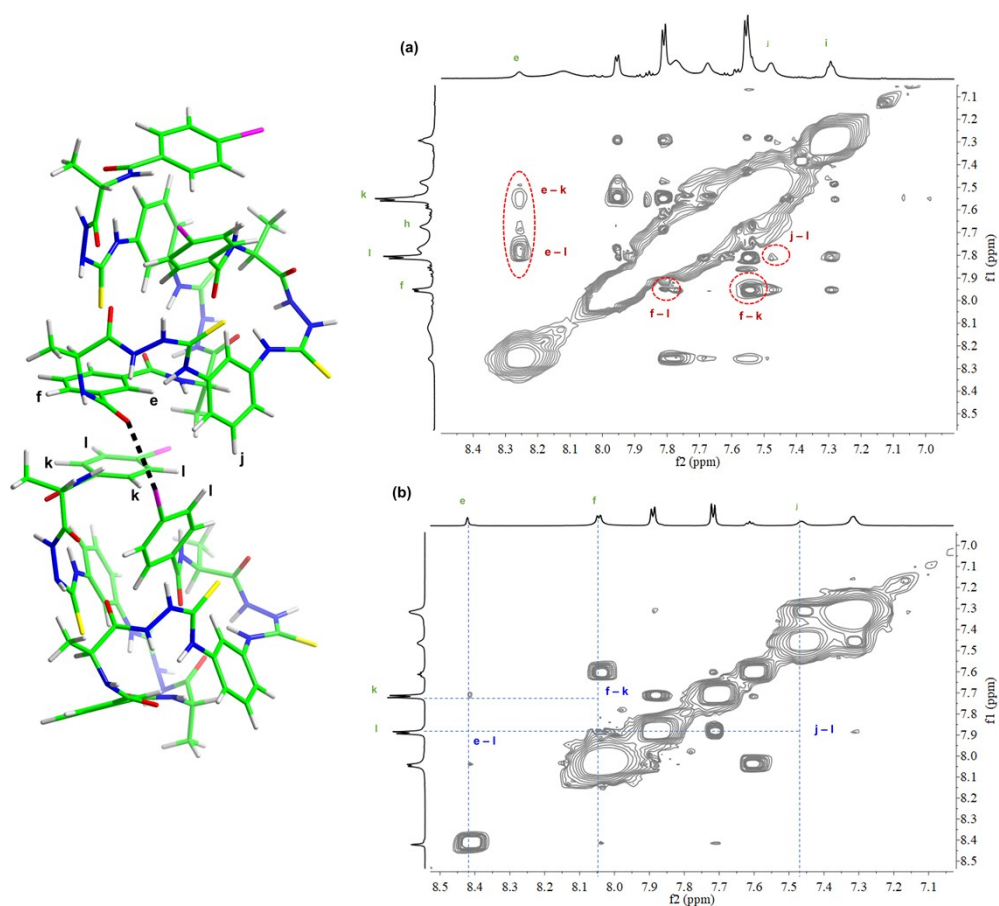


**Figure S21.** Expanded 2D NOESY spectra of **1L** in (a) 200:1 (v/v) CD<sub>3</sub>CN/DMSO-*d*<sub>6</sub> mixture and (b) DMSO-*d*<sub>6</sub> (850 MHz, 25 °C). [**1L**] = 200 μM. The proposed structure of the dimer of **1L** shows that two molecules are connected by C-I...O halogen bonding (dashed black line), allowing couplings of H<sup>e</sup>-H<sup>k</sup>, H<sup>e</sup>-H<sup>l</sup>, H<sup>f</sup>-H<sup>k</sup>, H<sup>f</sup>-H<sup>l</sup> and H<sup>j</sup>-H<sup>l</sup>.



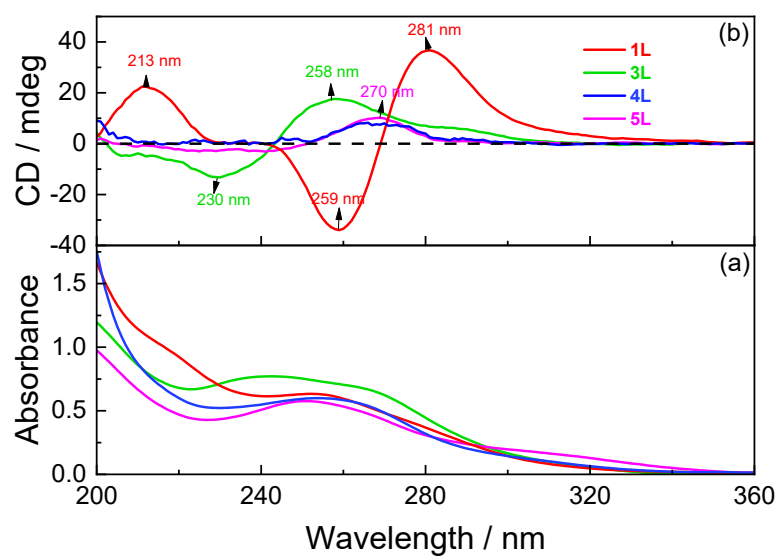


**Figure S22.** Absorption (a) and CD (b) spectra of **1L**, **3L**, **4L** and **5L** in CH<sub>3</sub>CN. [**1L**] = [**3L**] = [**4L**] = [**5L**] = 10  $\mu$ M.

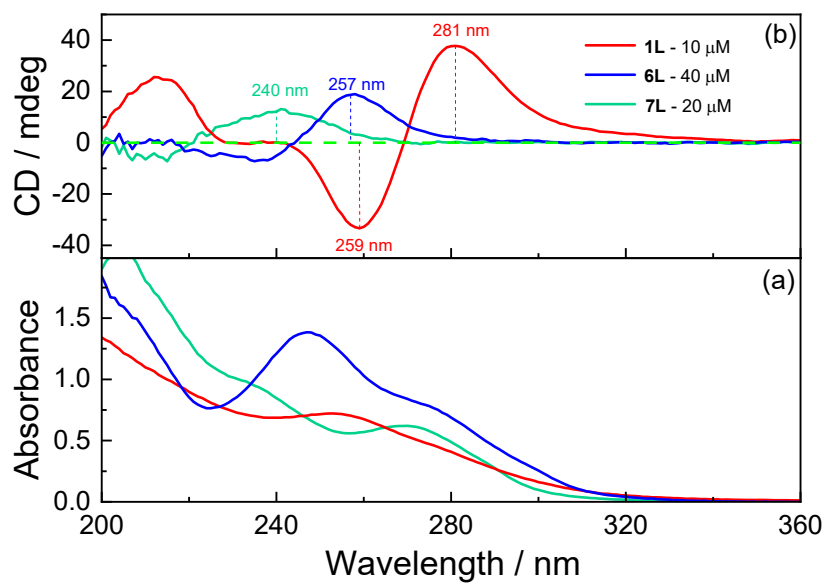


**Figure S23.** Absorption (a) and CD (b) spectra of **1L**, **6L** and **7L** in CH<sub>3</sub>CN. [**1L**] = 10  $\mu$ M, [**6L**] = 40  $\mu$ M and [**7L**] = 20  $\mu$ M.

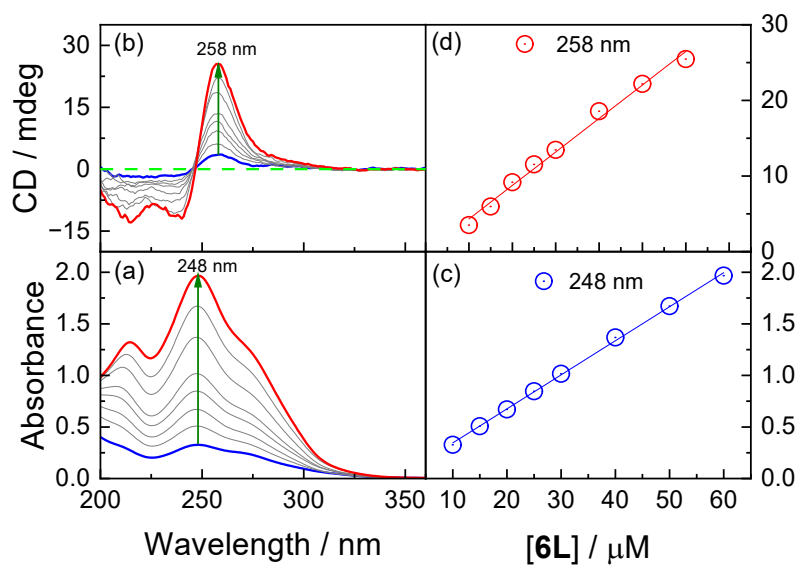


**Figure S24.** Concentration-dependent absorption (a) and CD (b) spectra of **6L** in  $\text{CH}_3\text{CN}$  and plots of absorbance at 248 nm (c) and CD signal at 258 nm (d) versus concentration of **6L** over 10 to 60  $\mu\text{M}$ .

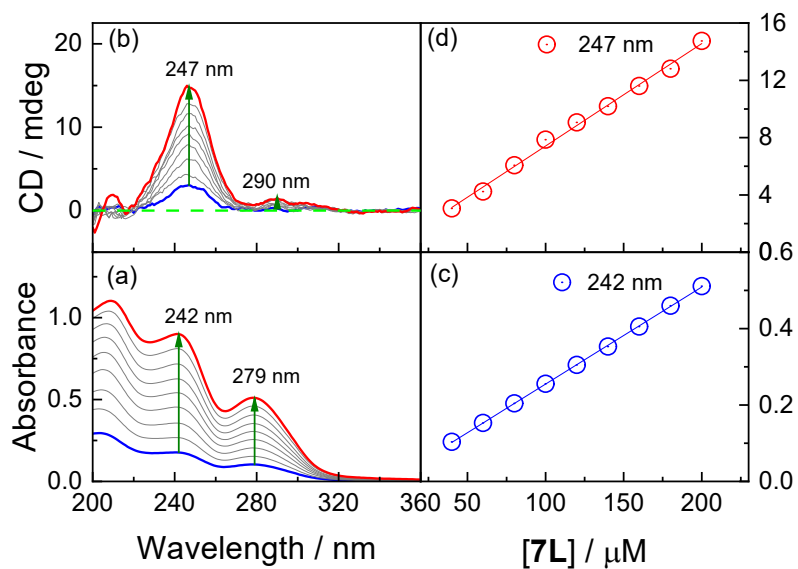


**Figure S25.** Concentration-dependent absorption (a) and CD (b) spectra of **7L** in  $\text{CH}_3\text{CN}$  and plots of absorbance at 242 nm (c) and CD signal at 247 nm (d) versus concentration of **7L** over 40 to 200  $\mu\text{M}$ .

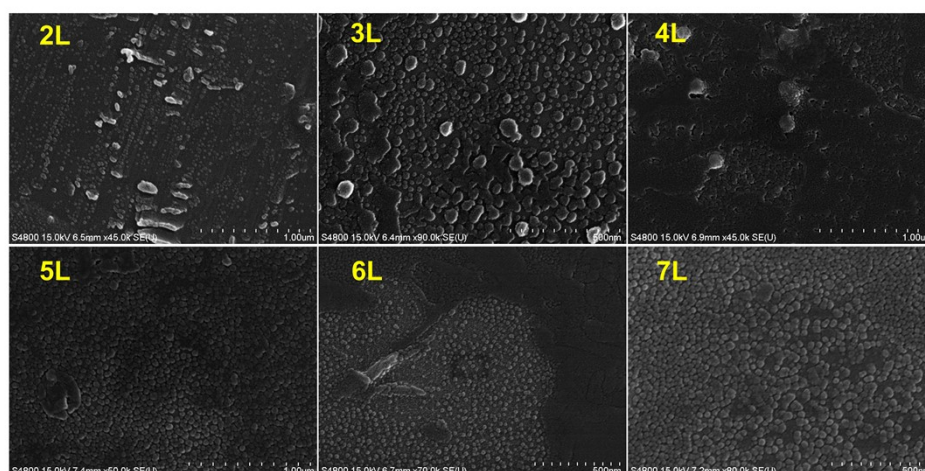


**Figure S26.** SEM images of air-dried samples of **2L**, **3L**, **4L**, **5L**, **6L** and **7L** in  $\text{CH}_3\text{CN}$  on platinum coated silicon wafers. Concentrations of **2L**-**7L** are  $10\ \mu\text{M}$ .

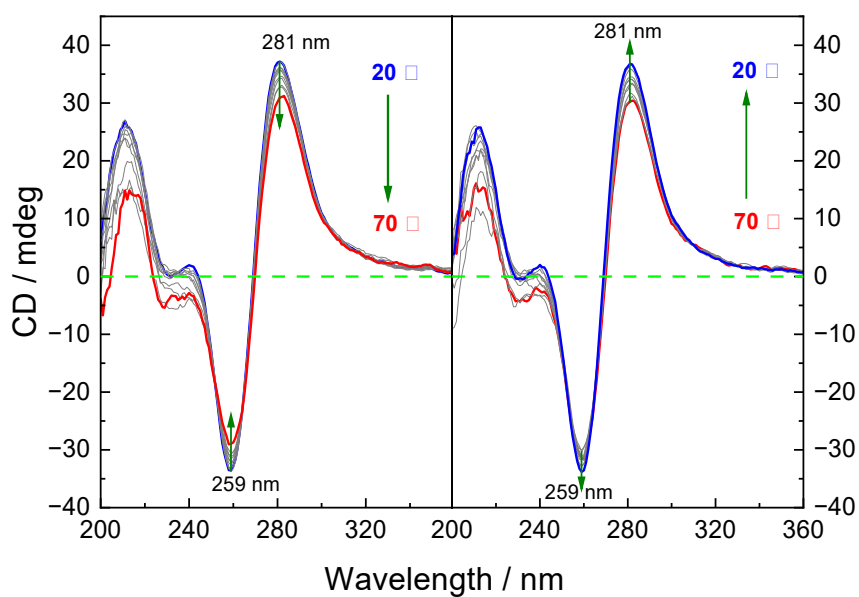


**Figure S27.** Temperature-dependent CD spectra of **1L** in  $\text{CH}_3\text{CN}$ .  $[\mathbf{1L}] = 10\ \mu\text{M}$ .

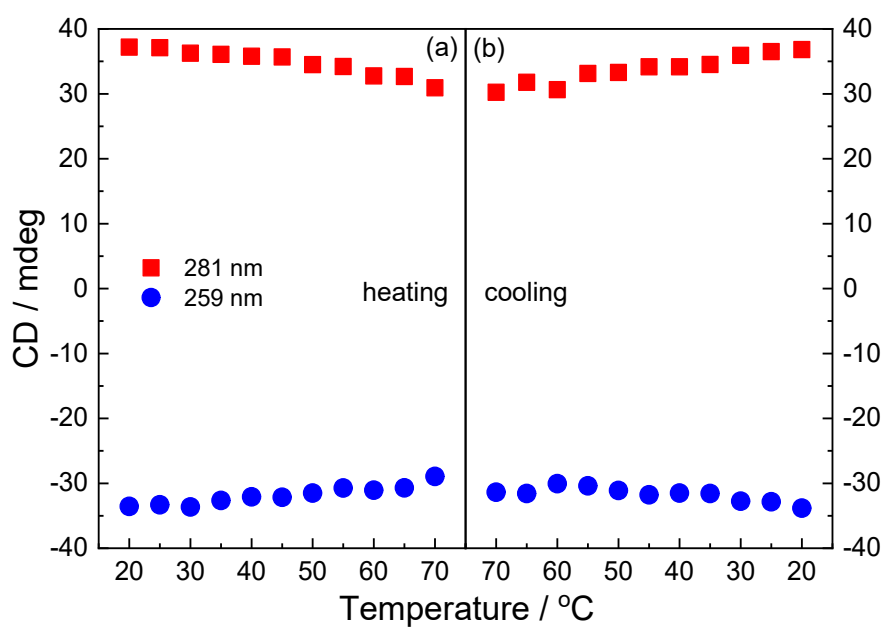


**Figure S28.** Temperature-dependent CD signals at 259 nm and 281 nm of **1L** in  $\text{CH}_3\text{CN}$  in the heating (a) and next cooling (b) processes. [**1L**] = 10  $\mu\text{M}$ .

#### 4. $^1\text{H}$ NMR and $^{13}\text{C}$ NMR spectra

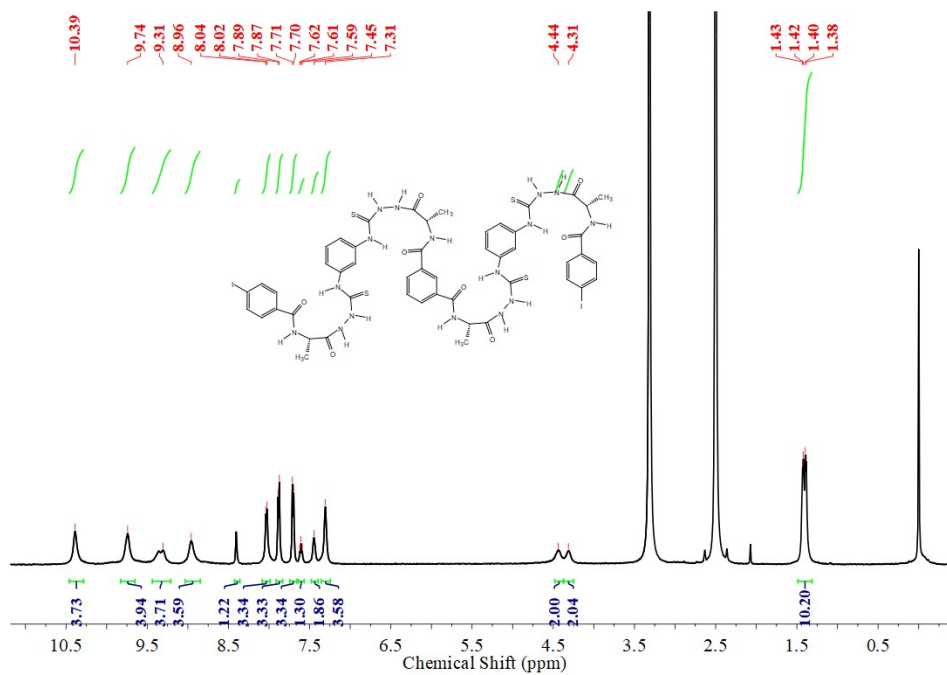


**Figure S29.** 500 MHz  $^1\text{H}$  NMR spectrum of **1L** in  $\text{DMSO}-d_6$ .

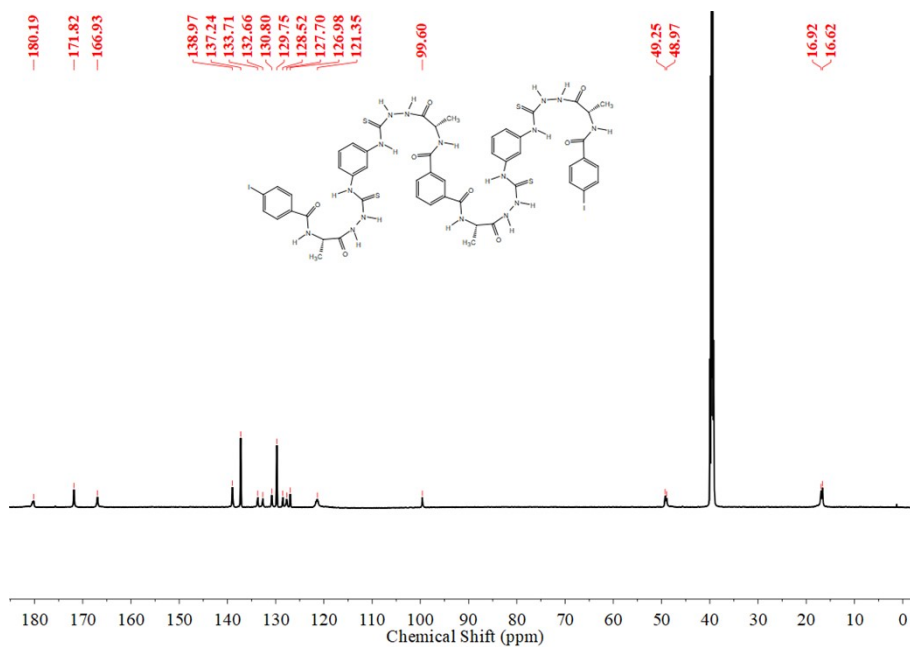


**Figure S30.** 214 MHz  $^{13}\text{C}$  NMR spectrum of **1L** in  $\text{DMSO}-d_6$ .

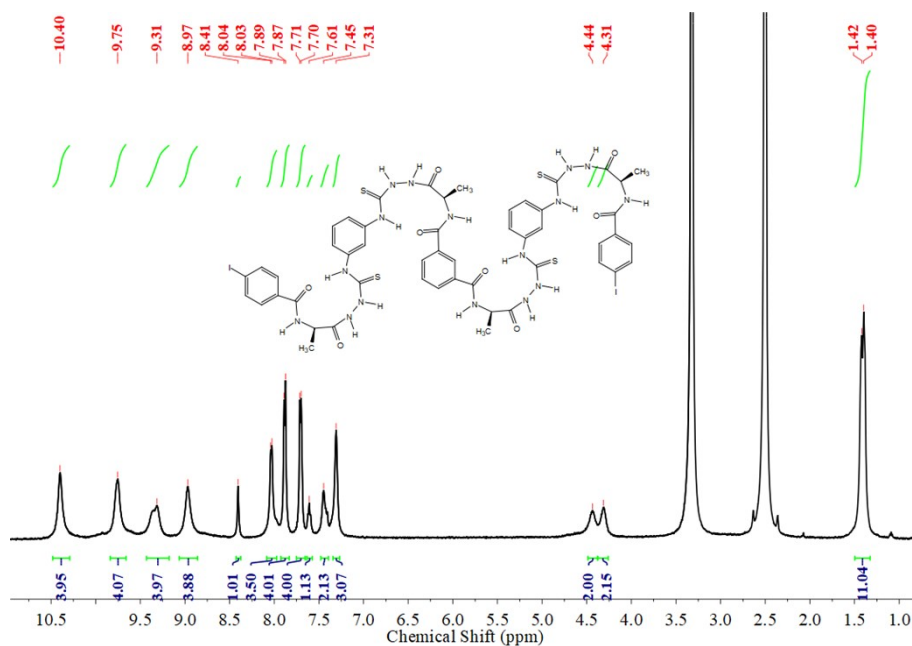


**Figure S31.** 500 MHz  $^1\text{H}$  NMR spectrum of **1D** in  $\text{DMSO}-d_6$ .

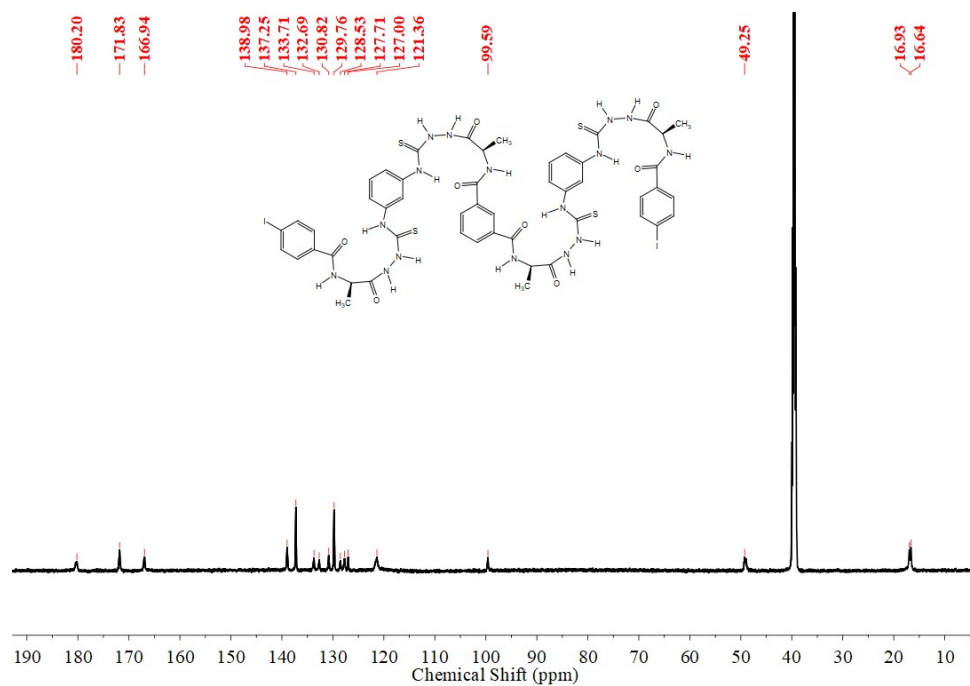


**Figure S32.** 214 MHz  $^{13}\text{C}$  NMR spectrum of **1D** in  $\text{DMSO}-d_6$ .

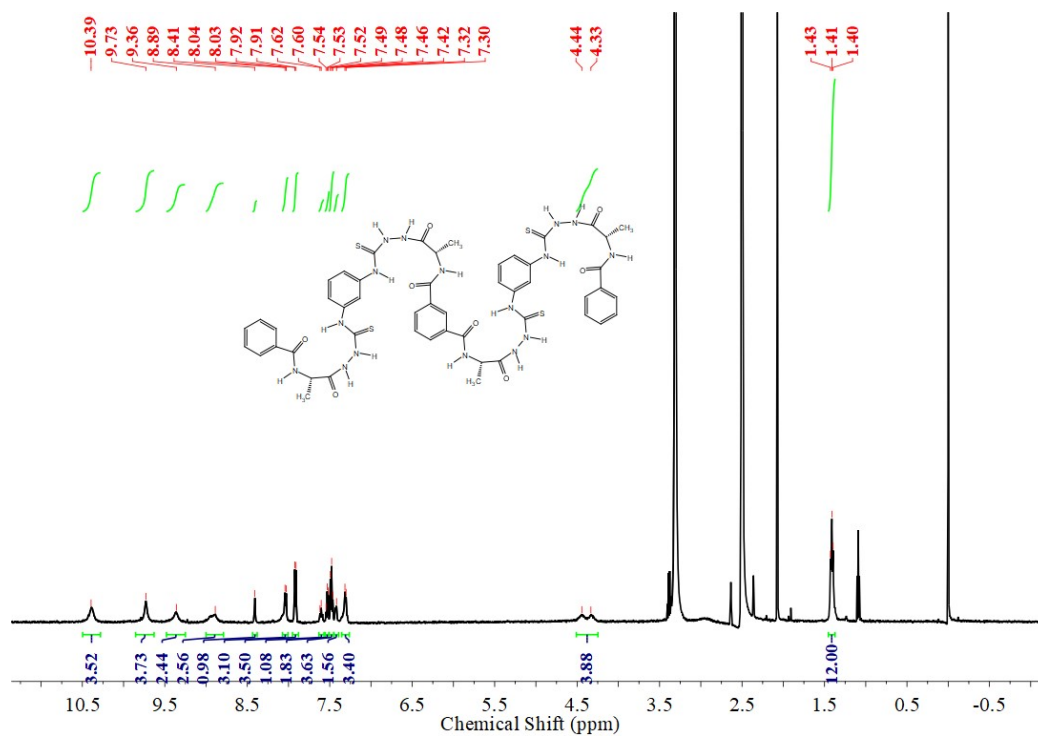


**Figure S33.** 500 MHz  $^1\text{H}$  NMR spectrum of **2L** in  $\text{DMSO-}d_6$ .

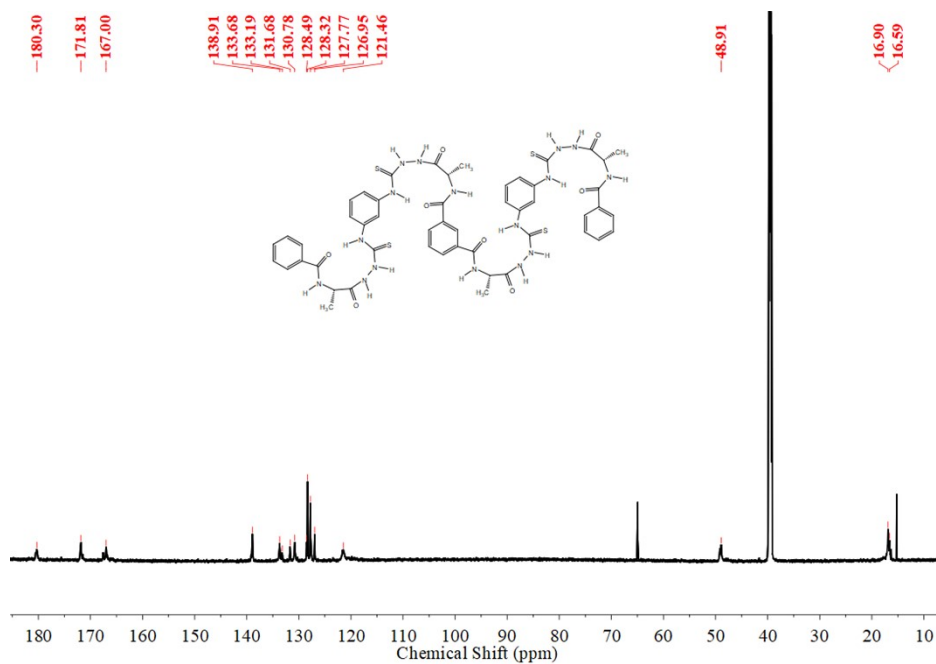


**Figure S34.** 214 MHz  $^{13}\text{C}$  NMR spectrum of **2L** in  $\text{DMSO-}d_6$ .

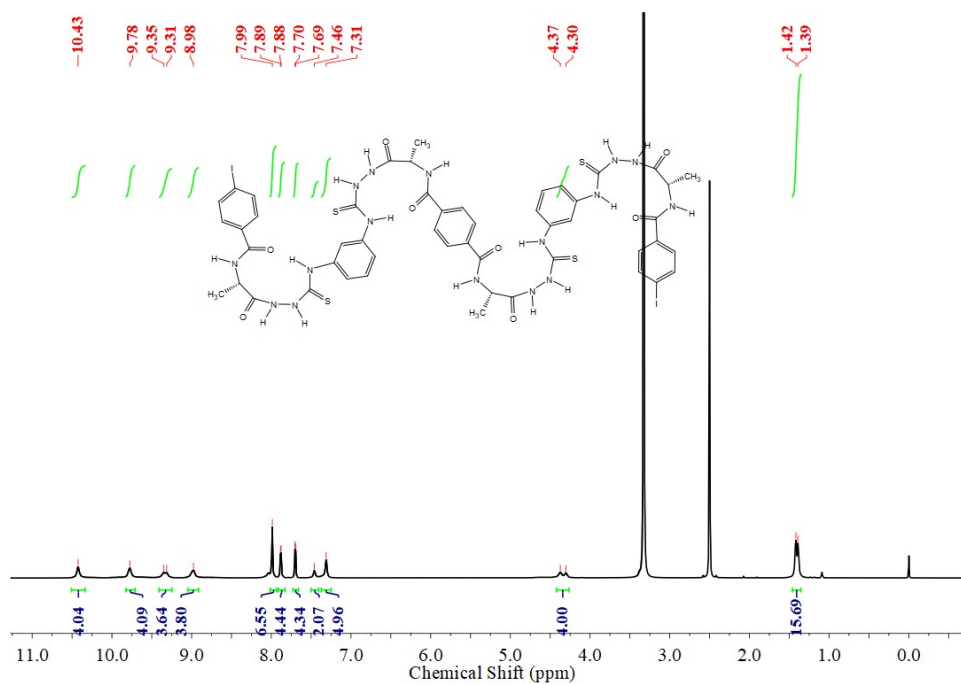


**Figure S35.** 500 MHz  $^1\text{H}$  NMR spectrum of **3L** in  $\text{DMSO}-d_6$ .

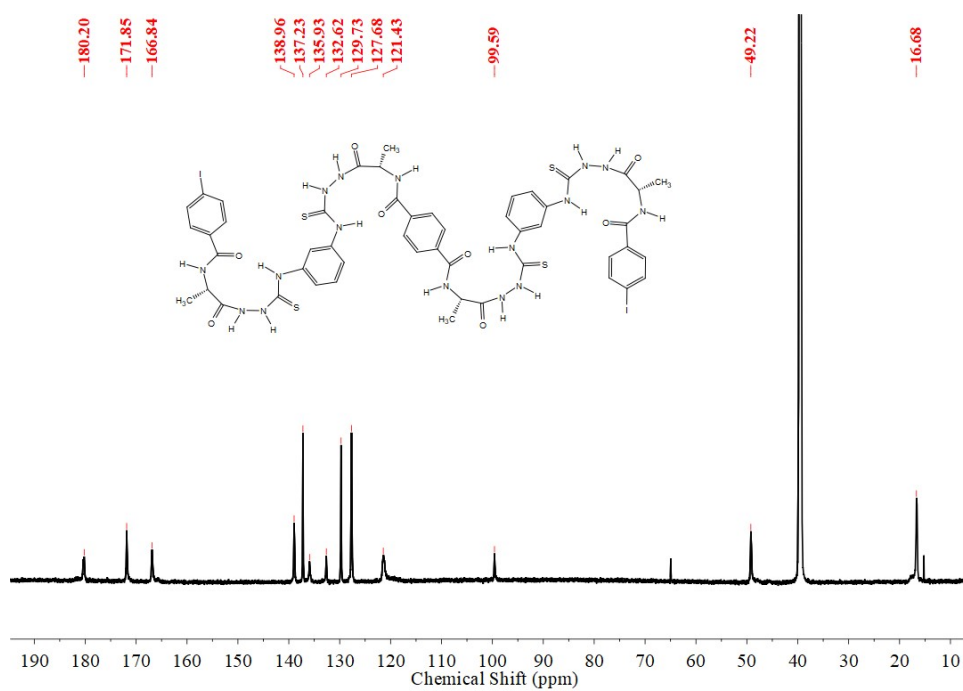


**Figure S36.** 214 MHz  $^{13}\text{C}$  NMR spectrum of **3L** in  $\text{DMSO}-d_6$ .



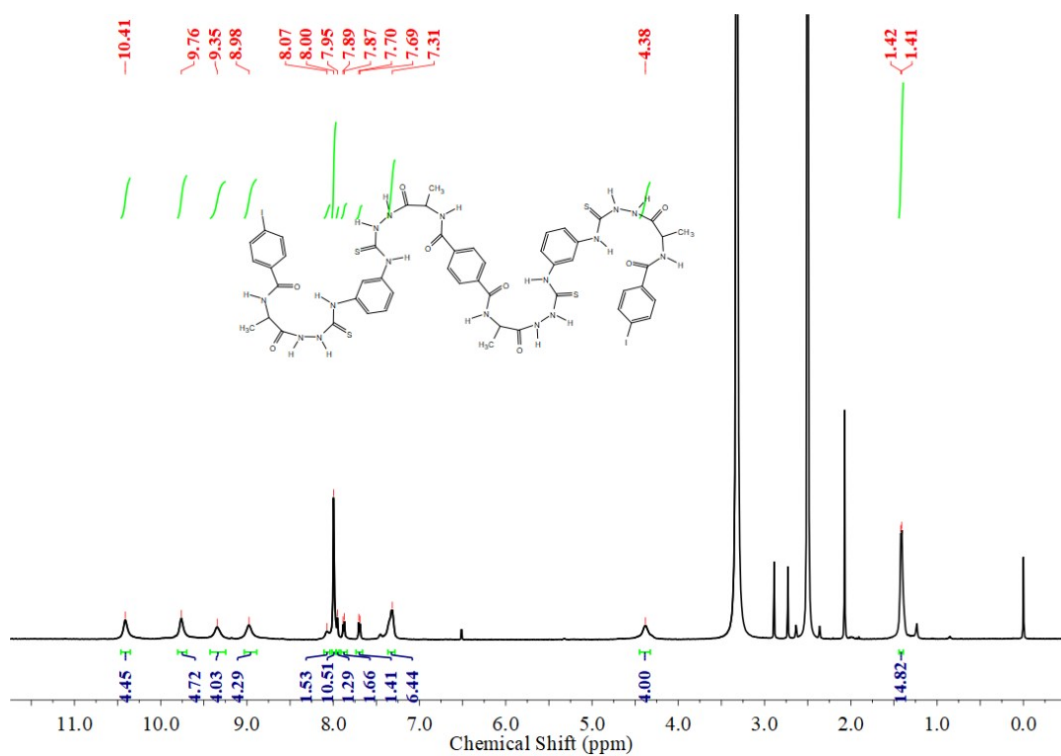


Figure S37. 500 MHz  $^1\text{H}$  NMR spectrum of **4L** in  $\text{DMSO}-d_6$ .

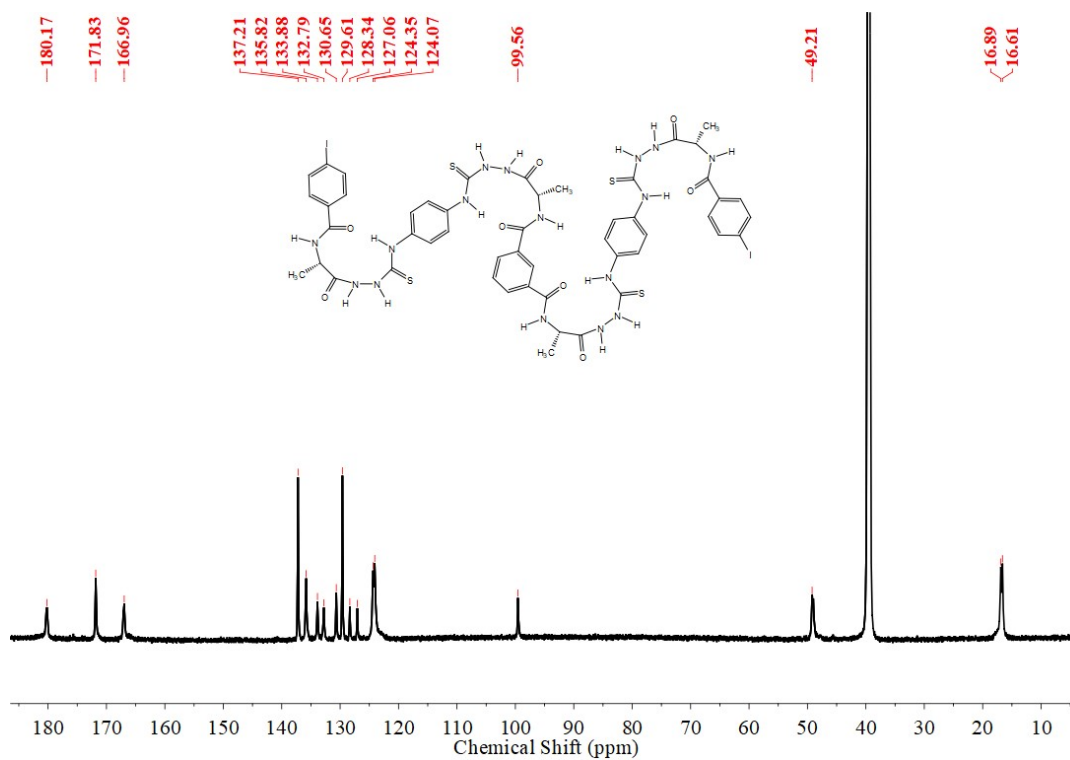
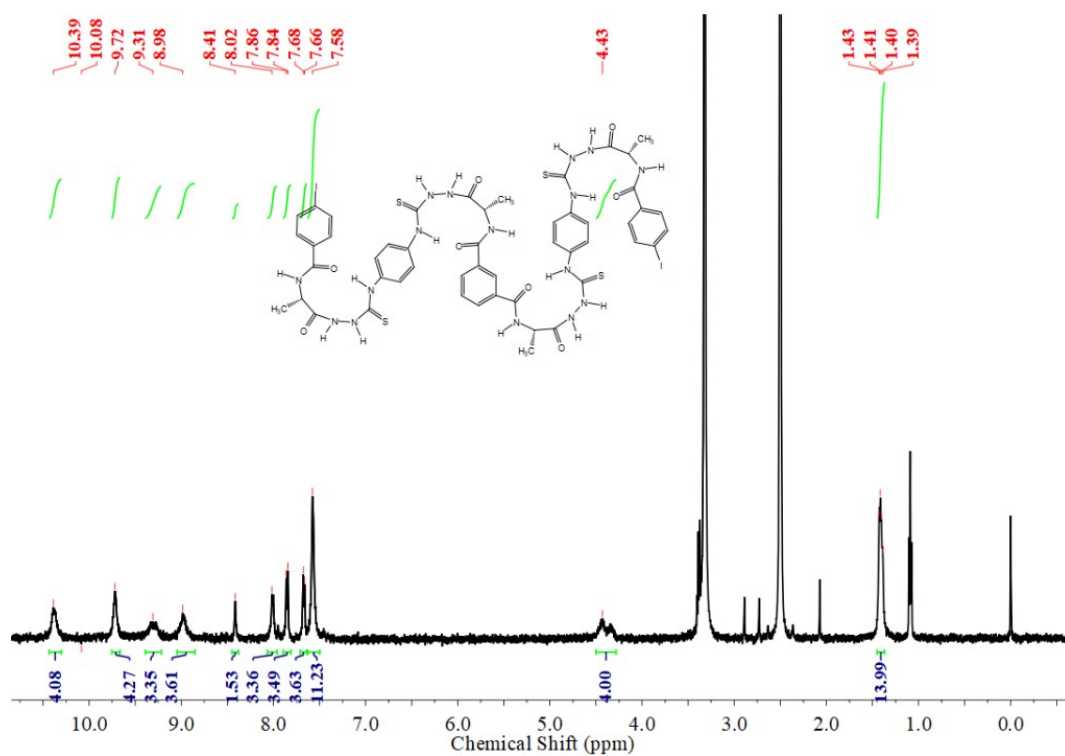
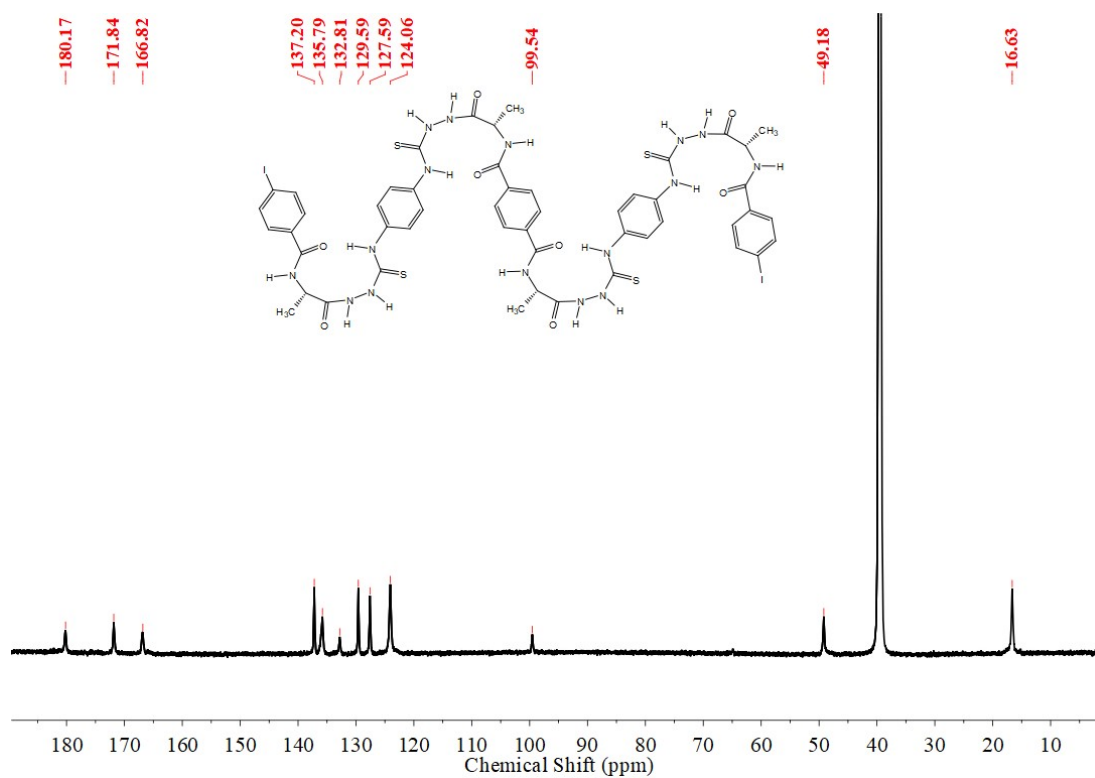


Figure S38. 214 MHz  $^{13}\text{C}$  NMR spectrum of **4L** in  $\text{DMSO}-d_6$ .



**Figure S39.** 500 MHz  $^1\text{H}$  NMR spectrum of **5L** in  $\text{DMSO}-d_6$ .



**Figure S40.** 214 MHz  $^{13}\text{C}$  NMR spectrum of **5L** in  $\text{DMSO}-d_6$ .

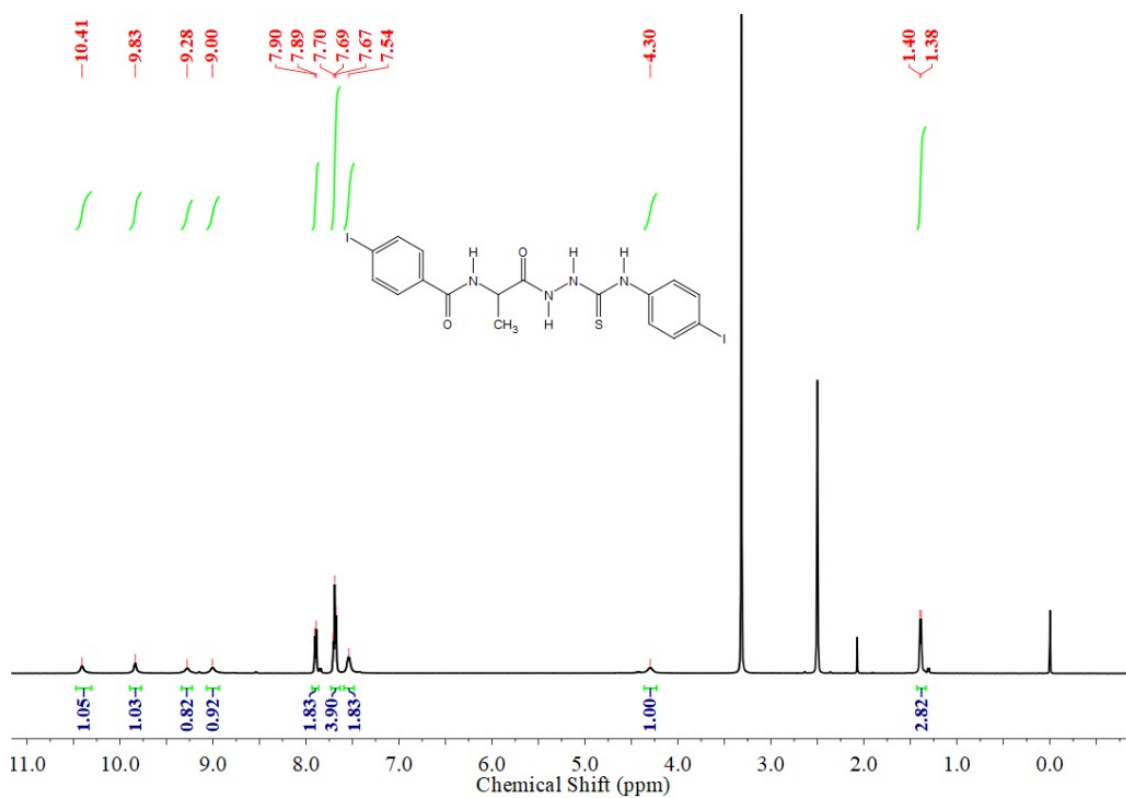


**Figure S41.** 500 MHz  $^1\text{H}$  NMR spectrum of **6L** in  $\text{DMSO}-d_6$ .

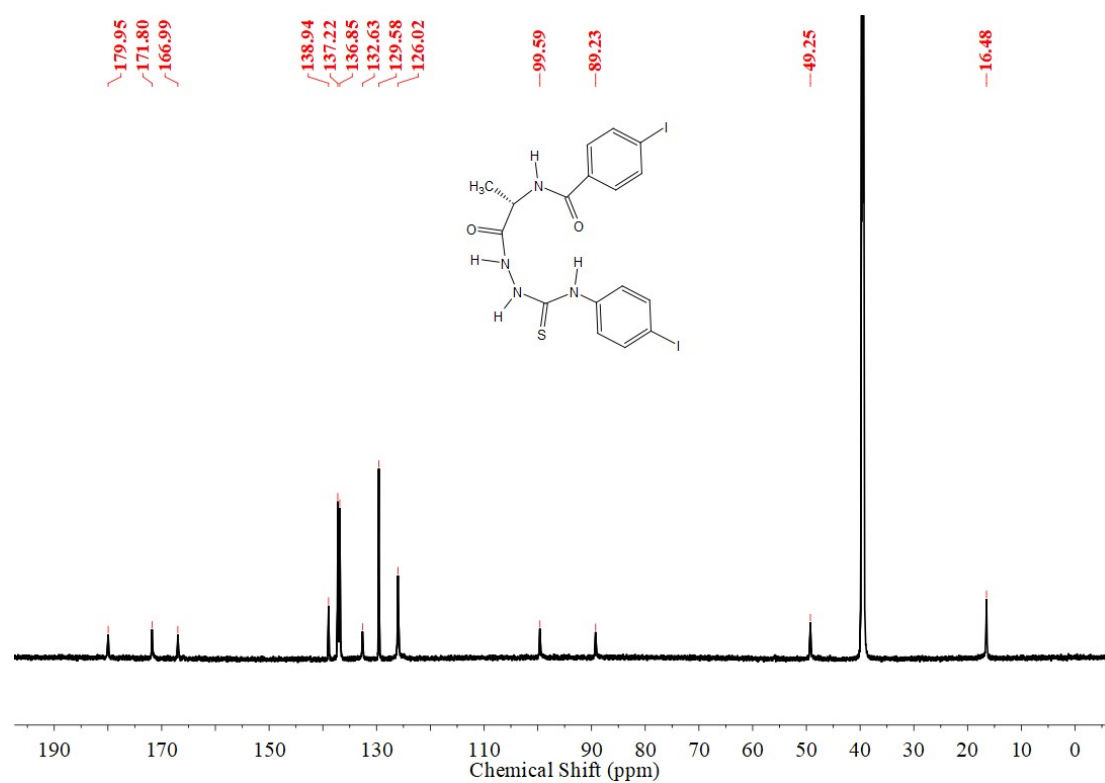


**Figure S42.** 214 MHz  $^{13}\text{C}$  NMR spectrum of **6L** in  $\text{DMSO}-d_6$ .

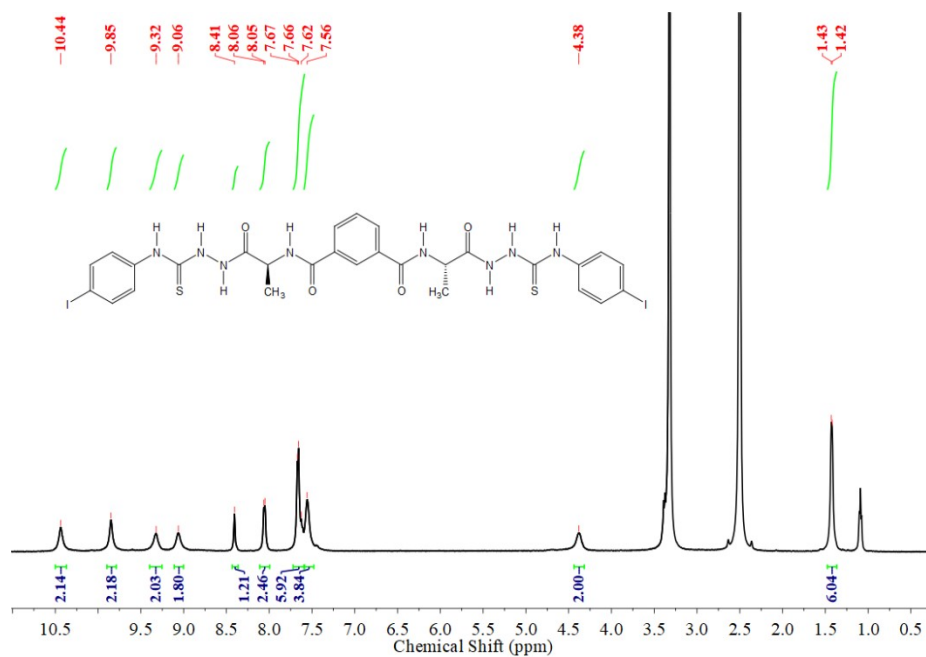


**Figure S43.** 500 MHz  $^1\text{H}$  NMR spectrum of **7L** in  $\text{DMSO}-d_6$ .

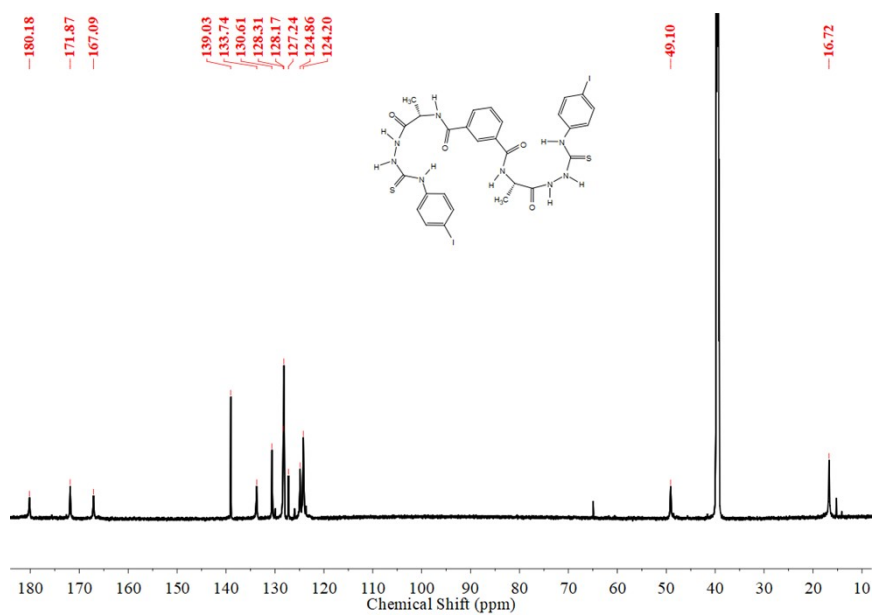


**Figure S44.** 214 MHz  $^{13}\text{C}$  NMR spectrum of **7L** in  $\text{DMSO}-d_6$ .